

# Study of Compound Particle Production in $^{28}\text{Si}$ and $^{32}\text{S}$ -Emulsion Collisions at 14.6 and 200 AGeV

Mir Hashim Rasool<sup>1\*</sup>, Mohammad Ayaz Ahmad<sup>2</sup>, Muzamil Ahmad Bhat<sup>1</sup>, Shafiq Ahmad<sup>1</sup>

<sup>1</sup>Department of Physics, Aligarh Muslim University, Aligarh, India

<sup>2</sup>Physics Department, Faculty of Science, University of Tabuk, Tabuk, Saudi Arabia

Email: [hrasool23@gmail.com](mailto:hrasool23@gmail.com)

Received 1 May 2015; accepted 24 July 2015; published 27 July 2015

Copyright © 2015 by authors and Scientific Research Publishing Inc.

This work is licensed under the Creative Commons Attribution International License (CC BY).

<http://creativecommons.org/licenses/by/4.0/>



Open Access

---

## Abstract

This work displays a study of the compound multiplicity characteristics of 14.6 and 200 AGeV/c  $^{28}\text{Si}$  and  $^{32}\text{S}$ -emulsion interactions, where the number of shower and grey particles taken together is termed as compound multiplicity,  $N_c$ . It has been found that the average compound multiplicity depends on the mass number of the projectile,  $A_p$ , and energy of the projectile. A positive linear dependence of the compound multiplicity on the black, grey, heavy and shower particles has been found. Also the scaling of compound multiplicity distributions produced in these interactions has been studied in order to check the validity of KNO-scaling. A simplified universal function has been used to represent the experimental data. The experimental results have been compared with those obtained by analyzing events generated with the computer code FRITIOF based on Lund Monte Carlo model.

## Keywords

Relativistic Heavy Ion Collision, Compound Particle Multiplicity, KNO Scaling, FRITIOF Model

---

## 1. Introduction

The study of relativistic heavy-ion collisions has provided new avenues in the field of high energy physics for giving information about the mechanism of particle production. It is important to achieve complete information regarding the mechanism of particle production in nucleus-nucleus collisions. When an energetic projectile collides with targets of nuclear emulsion, a number of charged and uncharged particles are produced. The emer-

---

\*Corresponding author.

gence of these particles occurs in a very short time and after this the nucleus remains excited for quite a long time on nuclear scale. The nucleus then de-excites resulting in the emission of a large number of nucleons and other heavy fragments.

The multiplicity of charged particles in high energy nucleus-nucleus interactions is an important parameter which indicates how many particles are produced in that interaction. The multiplicity distributions of produced particles help in learning the interaction mechanism. Generally, it is accepted that in high energy nucleus-nucleus collisions, the emission of fast target associated particles mostly the knocked out protons known as grey particles, takes place at a relatively latter stage of the collision. These fast protons with range  $L \geq 3$  mm and relative velocity  $0.3 \leq \beta \leq 0.7$  lie in the energy range 30 to 400 MeV. Moreover, these grey particles ( $N_g$ ) are often assumed to be the measure of the number of encounters made by the incident hadron inside the target nucleus [1]. Also the particles produced in the first stage of collision with relative velocity  $\beta \geq 0.7$  are known as relativistic shower particles ( $N_s$ ). These particles are mostly pions with a small admixture of charged K-mesons and fast protons. The analysis of the experimental data in terms of multiplicity distributions for grey and shower particles collectively known as compound multiplicity (*i.e.*  $N_c = N_g + N_s$ ) introduced by Jurak and Linscheid [2] is one of the main sources of information about the mechanism of particle production. Many workers [3]–[10] analyzed the data on nucleus-nucleus (AA) and hA collisions to investigate some interesting features of compound multiplicity distribution. But fewer attempts have been made to study the compound multiplicity distribution for  $^{28}\text{Si}$  and  $^{32}\text{S}$  with nuclear emulsion at 14.6 and 200 AGeV respectively. Keeping this fact in mind an effort is made in this direction.

We compare the experimental results with those obtained by analyzing events generated with the computer code FRITIOF based on Lund Monte Carlo model [11] [12] for high energy nucleus-nucleus interaction. The model assumes that, as the two nucleons collide with each other, particle production takes place through the creation of longitudinally excited strings between the constituents of same nucleon that subsequently fragment and new hadrons originate. The FRITIOF model mainly constitutes the inelastic hadron-hadron (h-h) collisions. Particle production goes through states of resonance created in Nucleon-Nucleon (NN) reaction at low energies whereas, at high energy, it proceeds through continuum spectra. The FRITIOF model assumes that all h-h interactions are binary reactions,  $h_1 + h_2 \rightarrow h'_1 + h'_2$ , where  $h'_1$  and  $h'_2$  are the excited states of the hadrons with continuous mass spectra. If one of the hadrons is in the ground state ( $h_1 + h_2 \rightarrow h_1 + h'_2$ ) the reaction is called “single diffraction dissociation”, otherwise it is non-diffractive interaction. The excited hadrons are considered as QCD-strings. A sampling of the string masses is the main constituent of the FRITIOF model. In principle, the mass sampling threshold can be below hadron mass. In the model it equals the ground state masses. The kinematic energy-momentum conservation law is applied through the excitation system in h-h collision. In case of h-A interactions, the FRITIOF model presumes that the string that originated from the projectile can interact with various intra-nuclear nucleons. Then it goes into a highly excited state. In this case, the same kinematics of h-h collisions is applied for the first collision of the projectile with one of the target nucleons. For the second collision analogous kinematics are used, considering the change in the mass of the hadrons and in the longitudinal momenta. As a result, consequent collisions will involve a systematically increasing mass of the hadron, if the transverse momentum transfers are small. A similar approach in kinematic conservation laws is also applied to simulate A-A interactions. Accordingly the mentioned kinematics in the longitudinal momentum conservation law is changed.

The modified FRITIOF code used in present work is based on version 1.6 (10 June 1986) of authors B Nilsson-Almqvist and Evert Stenlund, University of Lund, Lund, Sweden [11] [12]. The modification was carried out by V. V. Uzhinskii, LIT, JINR, Dubna, Russia, in 1995. A large sample of 5000  $^{32}\text{S}$ -emulsion events has been generated using the code, where the proportional abundance of different categories of target nuclei present in the emulsion material has been taken into account.

In this paper, we present our experimental results on the compound multiplicity of grey and shower particles taken together and their characteristics with respect to other emitting particles in inelastic collision of  $^{28}\text{Si}$  and  $^{32}\text{S}$  with nuclear emulsion at 14.6 and 200 AGeV respectively. Also the scaling of compound multiplicity distributions produced in these interactions has been studied in order to check the validity of KNO-scaling. A simplified universal function has been used to represent the experimental data.

## 2. Experimental Techniques

In this experiment two stacks of Ilford G5 nuclear emulsion plates exposed horizontally to a  $^{32}\text{S}$ -beam at 200

AGeV from Supper Proton Synchrotron, SPS at CERN have been utilized for data collection. The scanning of the plates is performed with the help of Leica DM2500M microscope with a 10× objective and 10× ocular lens provided with semi-automatic scanning stages. The method of line scanning was used to collect the inelastic  $^{32}\text{S}$ -Em interactions. The interactions collected from line scanning were scrutinized under an optical microscope (Semi-Automatic Computerized, Leica DM6000M) with a total magnification of  $10 \times 100$  using 10× eyepiece and 100× oil immersion objective. The measuring system associated with it has  $1\mu\text{m}$  resolution along X and Y axes and  $0.5\mu\text{m}$  resolution along the Z-axis.

Also two Stacks of FUJI type emulsion exposed horizontally to a 14.6 AGeV  $^{28}\text{Si}$ -beam at the Alternating Gradient Synchro-Phasotron (AGS) of Brookhaven National Laboratory (BNL), New York, USA have been utilized for the data collection. A Japan based NIKON microscope with 8 cm movable stage using 40× objectives and 10X eyepieces has been used to scan the plates. In the present study, the method of line scanning has been used to pick up the interaction stars. Each plate was scanned by two independent observers to increase the scanning efficiency. The final measurements were done using an oil immersion 100× objective.

The tracks associated with the interactions are classified in accordance with their ionization, range and velocity into following groups [13] [14].

**i) Shower Tracks:** The tracks having specific ionization  $g^* (= g/g_0) < 1.4$  and relative velocity  $\beta > 0.7$  are taken as shower tracks, where  $g_0$  is the Fowler and Perkins parameter [15] for plateau ionization of relativistic particles. The grain density is defined as the number of grains per unit path length. The density of the developed grains depends on the charge and velocity of the particle, which is a function of ionization loss of that particle. However, it is observed that the grain density,  $g$ , is affected by the degree of development of emulsion. Therefore, in order to obtain an accurate value of ionization a parameter known as specific ionization ( $g^* = g/g_0$ ) is obtained by dividing it with the minimum ionization singly charged particle ( $g_0$ ) lying in the same region of emulsion. The number of such tracks in an event is represented by “ $N_s$ ”. Shower tracks producing particles are mostly pions, with small admixture of charged K-mesons and fast protons. These particles are mostly produced in a forward cone. Because of high velocity these particles are not generally confined with the emulsion pellicle. Since they have minimum ionization so are the most energetic. Their energy is in GeV range.

**ii) Grey Tracks:** The secondary tracks having specific ionization in the interval  $1.4 < g^* \leq 10$  are known as grey tracks. The numbers of such tracks in a star are designated by ‘ $N_g$ ’. This corresponds to protons with velocity in the interval  $0.3 \leq \beta \leq 0.7$  and range  $\geq 3.0$  mm in emulsion. Grey tracks are associated with the recoiling protons and have energy range (30 - 80) MeV. The sum of the number of grey and shower tracks in such an interaction is known as compound particle multiplicity and their number in a collision is represented by  $N_c = N_g + N_s$ .

**iii) Blacks Tracks:** Black tracks consist of both singly and multiply charged fragments emitted from excited target. They are fragments of various elements like carbon, lithium, beryllium etc. with specific ionization  $g^* > 10$ . These black particles have the maximum ionizing power. So they are less energetic and consequently are short ranged. Ranges of black particles are less than 3 mm in the emulsion medium and have relative velocities  $\beta$  less than 0.3. In the emulsion experiments it is very difficult to measure the charge of the fragments. So identification of the exact nucleus is not possible.

**iv) Projectile fragments:** Besides these tracks there are few projectile fragments as well. In high-energy nuclear collisions the projectile beam which collides with the target nucleus also undergoes fragmentation. These particles have constant ionization, long range and small emission angle. They generally lie within  $3^\circ$  with respect to the main beam direction. These projectile fragments must be identified with great care.

**v) Heavily Ionizing Tracks:** The black and grey tracks taken together are said to be heavily ionizing tracks. Thus these tracks correspond to  $g^* \geq 1.4$  or  $\beta \leq 0.7$ . Their number in a star,  $N_h = (N_b + N_g)$  is a characteristics of the target.

There is a limitation with nuclear emulsion that the exact identification of target is not possible since the medium of the emulsion is heterogeneous and composed of H, C, N, O, Ag and Br nuclei. The events produced due to the collisions with different targets in nuclear emulsion are usually classified into three main categories on the basis of the multiplicity of heavily ionizing tracks in it.

The events with  $N_h \leq 1$  are classified as collisions with hydrogen (H,  $A_T = 1$ ),  $2 \leq N_h \leq 7$  are classified as collision with group of light nuclei (CNO,  $\langle A_T \rangle = 14$ ) and  $N_h \geq 8$  are classified as collision with group of heavy nuclei (AgBr,  $\langle A_T \rangle = 94$ ) respectively. However, the grouping of events only on the basis of  $N_h$  values does not lead to the right percentage of events of interactions due to light and heavy group of nuclei. In fact, a considera-

ble fraction of stars with  $N_h \leq 7$  are produced in the interactions with heavy group of nuclei. Therefore we have used the following criteria [15] [16].

AgBr events:

- i)  $N_h > 7$ , or
- ii)  $N_h \leq 7$  and at least one track with rang  $R \leq 10 \mu\text{m}$  and no track with  $10 < R \leq 50 \mu\text{m}$

CNO events:

- i)  $2 \leq N_h \leq 7$  and no track with  $R \leq 10 \mu\text{m}$ .

H events:

- i)  $N_h = 0$ , or
- ii)  $N_h = 1$ , and no track with  $R \leq 50 \mu\text{m}$ .

### 3. Results and Discussions

#### 3.1. Compound Multiplicity Distributions at 14.6 and 200 AGeV

In order to check the role of target size dependence on the compound multiplicity, the present data are categorized into three groups of CNO, AgBr and Emulsion events.

The compound multiplicity distributions are plotted in **Figures 1(a)-(c)** and **Figures 2(a)-(c)** for  $^{28}\text{Si}$  and  $^{32}\text{S}$  projectiles at 14.6 and 200 AGeV respectively with different target groups *i.e.* CNO and AgBr and emulsion. It is evident from the figures that the compound multiplicity distributions for different target groups become wider with increasing target size for both  $^{28}\text{Si}$  and  $^{32}\text{S}$  projectiles. Also it is observed that the peaks of distribution shifts towards higher  $N_c$  values in  $^{32}\text{S}$  as compared to  $^{28}\text{Si}$ . This indicates that the more compound particles are being produced with increasing projectile mass number and energy of projectile nucleus, thereby confirming conversion of energy into mass. Similar results were obtained by other workers [5]-[10] of different projectiles at different energies.

The experimental results are compared with the FRITIOF generated events and the results are also shown in **Figures 1(a)-(c)** and **Figures 2(a)-(c)** for  $^{28}\text{Si}$  and  $^{32}\text{S}$  projectiles at 14.6 and 200 AGeV respectively. This indicates that the FRITIOF model reproduces satisfactorily the  $N_s$ ,  $N_g$ , and  $N_c$ -multiplicity distributions and thus exhibit a similar and consistent behaviour as discussed in the experimental results. Thus, there is a good justification to reproduce the overall compound multiplicity distribution by the considered code of the FRITIOF.

The average values of compound multiplicity,  $\langle N_c \rangle$ , of present experimental data along with the corresponding FRITIOF data (given in parenthesis in **Table 1**) for different projectiles at different energies [17]-[20] are presented in **Table 1**, which clearly exhibits that the average compound multiplicity increases with mass number and energy of the projectiles. The average values of compound multiplicity  $\langle N_c \rangle$ , its dispersion  $D(N_c) \{= (\langle N_c^2 \rangle - \langle N_c \rangle^2)^{1/2}\}$  and the ratio  $\langle N_c \rangle / D(N_c)$  are given in **Table 2** for different projectiles as well as for different emul-

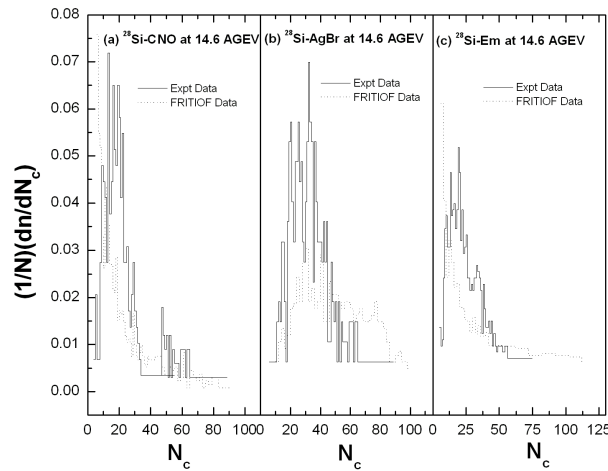


**Figure 1.** Compound multiplicity distributions for different emulsion targets in  $^{28}\text{Si}$  at 14.6 AGeV with nuclear emulsion interactions.

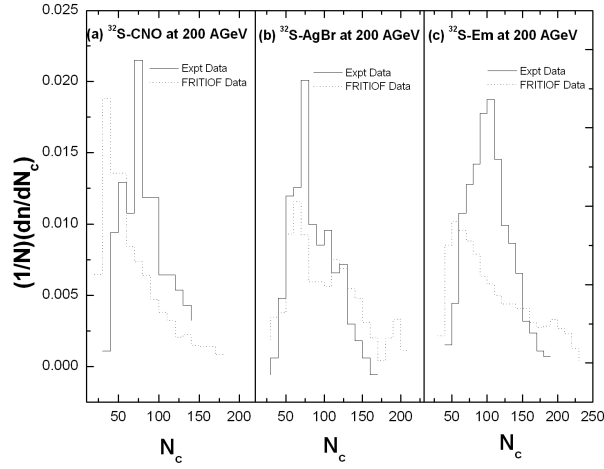


**Figure 2.** Compound multiplicity distributions for different emulsion targets in  $^{32}\text{S}$  at 200 AGeV with nuclear emulsion interactions.

**Table 1.** The mean values of compound multiplicities  $\langle N_c \rangle$  for different projectiles with nuclear emulsion.

Energy/Nucleon AGeV	Collision Type	$\langle N_c \rangle$	Ref.
2.1	$^{14}\text{N}$ -Em	$14.10 \pm 0.42$	[20]
2.1	$^{56}\text{Fe}$ -Em	$23.17 \pm 1.54$	[19]
3.7	$^{32}\text{S}$ -Em	$16.62 \pm 0.49$	[19]
4.5	$^{28}\text{Si}$ -Em	$21.97 \pm 1.23$	[17]
<b>14.6</b>	<b><math>^{28}\text{Si}</math>-Em</b>	<b><math>24.20 \pm 0.17</math></b> <b><math>(29.54 \pm 0.26)</math></b>	<b>Present Work</b>
60	$^{16}\text{O}$ -Em	$36.28 \pm 2.30$	[18]
200	$^{16}\text{O}$ -Em	$59.34 \pm 3.10$	[18]
<b>200</b>	<b><math>^{32}\text{S}</math>-Em</b>	<b><math>91.61 \pm 0.58</math></b> <b><math>(74.02 \pm 0.52)</math></b>	<b>Present Work</b>

**Table 2.** Values of  $\langle N_c \rangle$ ,  $D(N_c)$  and  $\langle N_c \rangle/D(N_c)$  for Different Nuclear Emulsion Targets in  $^{28}\text{Si}$  and  $^{32}\text{S}$  projectiles with nuclear emulsion at 14.6 and 200 AGeV along with corresponding FRITIOF predictions given in parenthesis.

Projectile	Target	$\langle N_c \rangle$	$D(N_c)$	$\langle N_c \rangle/D(N_c)$	References
$^{32}\text{S}$ at 200 AGeV	H	$77.10 \pm 1.96$ <b><math>(30.94 \pm 0.30)</math></b>	$23.32 \pm 1.12$ <b><math>(18.59 \pm 0.86)</math></b>	$3.30 \pm 0.25$ <b><math>(1.66 \pm 0.11)</math></b>	Present Study
	CNO	$83.28 \pm 0.96$ <b><math>(62.45 \pm 0.83)</math></b>	$23.64 \pm 1.11$ <b><math>(41.25 \pm 0.64)</math></b>	$3.52 \pm 0.16$ <b><math>(1.51 \pm 0.08)</math></b>	
	Em	$91.59 \pm 0.53$ <b><math>(74.02 \pm 0.64)</math></b>	$27.90 \pm 0.28$ <b><math>(53.33 \pm 0.54)</math></b>	$3.28 \pm 0.23$ <b><math>(1.38 \pm 0.10)</math></b>	
	AgBr	$96.34 \pm 0.66$ <b><math>(114.47 \pm 0.86)</math></b>	$27.36 \pm 0.42$ <b><math>(51.79 \pm 0.65)</math></b>	$3.52 \pm 0.05$ <b><math>(2.21 \pm 0.13)</math></b>	
	H	$13.05 \pm 0.37$ <b><math>(9.50 \pm 0.26)</math></b>	$4.13 \pm 0.25$ <b><math>(6.50 \pm 0.15)</math></b>	$2.15 \pm 0.19$ <b><math>(1.46 \pm 0.06)</math></b>	
$^{28}\text{Si}$ at 14.6 AGeV	CNO	$17.93 \pm 0.77$ <b><math>(17.54 \pm 0.22)</math></b>	$7.28 \pm 0.33$ <b><math>(15.58 \pm 0.23)</math></b>	$2.46 \pm 0.13$ <b><math>(1.12 \pm 0.05)</math></b>	Present Study
	Em	$23.89 \pm 0.18$ <b><math>(29.63 \pm 0.45)</math></b>	$13.44 \pm 0.11$ <b><math>(27.54 \pm 0.35)</math></b>	$1.82 \pm 0.02$ <b><math>(1.07 \pm 0.04)</math></b>	
	AgBr	$32.05 \pm 0.66$ <b><math>(46.77 \pm 0.33)</math></b>	$12.76 \pm 0.63$ <b><math>(24.65 \pm 0.25)</math></b>	$2.51 \pm 0.11$ <b><math>(1.89 \pm 0.09)</math></b>	
	H	$13.05 \pm 0.37$ <b><math>(9.50 \pm 0.26)</math></b>	$4.13 \pm 0.25$ <b><math>(6.50 \pm 0.15)</math></b>	$2.15 \pm 0.19$ <b><math>(1.46 \pm 0.06)</math></b>	
$^{12}\text{C}$ at 4.5 AGeV	Em	$16.17 \pm 0.18$	$10.51 \pm 0.34$	$1.54 \pm 0.06$	[23]
$^{24}\text{Mg}$ at 4.5 AGeV	Em	$19.00 \pm 0.34$	$16.00 \pm 0.24$	$1.18 \pm 0.75$	[24]

sion targets along with the corresponding FRITIOF data of the present work. It may be noticed from the table that the values of  $D(N_c)$  with different target groups are higher for  $^{32}\text{S}$  projectile as compared to other light projectiles. From these observations we may conclude that the complete disintegration of nuclei increases with increasing energy and mass of the projectile. However, as expected the values of  $\langle N_c \rangle / D(N_c)$  remains almost constant for different projectiles mass and energy, which does not agree with the cascade evaporation model [21] and gives strong support to model approaches which take into account details of space-time evolution in multi-particle production [22]. The value of this ratio is somewhat large in case of  $^{32}\text{S}$ -beam.

### 3.2. Variation of the Dispersion with the Average Compound Multiplicity

In order to investigate the variation of the dispersion  $D(N_i)$  with  $\langle N_i \rangle$ , a plot of dispersion  $D(N_i)$  as a function of average compound multiplicity,  $\langle N_c \rangle$  and the average shower multiplicity,  $\langle N_s \rangle$  for different emulsion interactions is shown in **Figure 3**. There exists a linear relation between dispersion and average value of  $N_i$ . The least square method has been utilized to obtain the following relation:

$$D(N_s) = (0.21 \pm 0.02) \langle N_s \rangle + (6.78 \pm 0.51) \quad (1)$$

$$D(N_c) = (0.22 \pm 0.01) \langle N_c \rangle + (7.70 \pm 0.87) \quad (2)$$

The following important features may be noted from the figure:

The linear relations of dispersion,  $D(N_i)$  with  $\langle N_s \rangle$  and  $\langle N_c \rangle$  indicates that the grey particles are of special interest due to the fact that they are emitted during, or shortly after, the passage of the leading particles. The experimental values corresponding to  $\langle N_c \rangle$  are taken from **Table 2** whereas the experimental values of  $\langle N_s \rangle$  corresponding to different projectiles are taken from references [17] [18] along with our results.

### 3.3. Variations of $\langle N_c \rangle$ with Projectile Masses ( $A_p$ ), Energy ( $E_p$ ) and Target Size ( $A_T$ )

In order to study the particle production dependence on the mass number of projectiles, we have plotted the variation of  $\langle N_c \rangle$  with the mass number of projectile ( $A_p$ ) [1] [23]-[29] in **Figure 4**. It may be observed from the figure that  $\langle N_c \rangle$  increases rapidly with increasing mass of the projectiles. The dependence of the average compound multiplicities on projectile mass number,  $A_p$ , has been studied using the following power law:

$$\langle N_c \rangle = K A_p^a \quad (3)$$

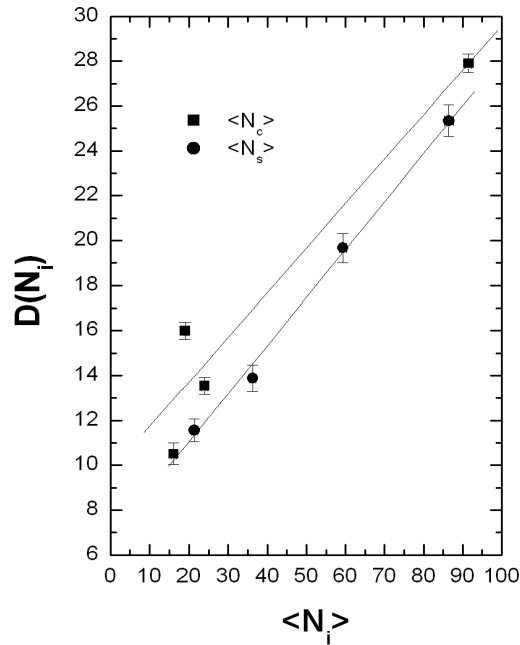


**Figure 3.** Variation of  $D(N_i)$  with  $\langle N_i \rangle$  ( $i = s, c$ ).

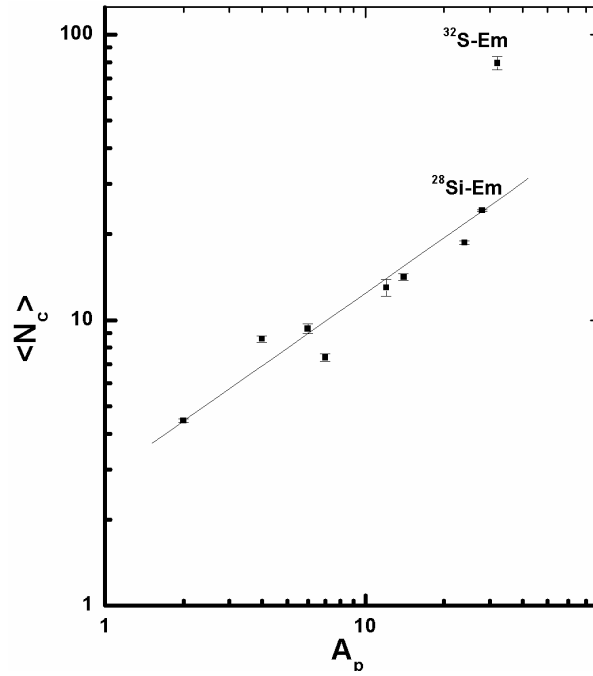


**Figure 4.** Dependence of  $\langle N_c \rangle$  on the mass number.

The above power law represents the experimental points satisfactorily and the values of  $K$  and  $\alpha$  obtained from the least square fit are found to be  $1.64 \pm 0.10$  and  $0.45 \pm 0.05$  respectively for the present data. The values of  $\alpha$  obtained by various workers [2] [6] [27] [30] for different projectiles are reported as  $0.44 \pm 0.03$ ,  $0.40 \pm 0.07$ ,  $0.47 \pm 0.07$ ,  $0.49 \pm 0.07$  respectively. Thus, these values are consistent with the value obtained in the present work. The compound multiplicity is nearly proportional to the linear dimension of the projectile nucleus upto  $A_p = 28$ . The strong dependence of the  $\langle N_c \rangle$  on the mass of the colliding nucleus are due to the increase in the overlapping region of the two interacting nuclei.

**Figure 5** shows the variation of  $\langle N_c \rangle$  with the energy of the projectiles. It has been found that the average compound multiplicity increase linearly with the energy of the projectile. The solid line in the **Figure 5** is the linear fit to the experimental data which exhibit a linear relation and the values of inclination coefficient and intercept are found as  $0.39 \pm 0.09$  and  $4.52 \pm 1.10$  respectively.

Also the dependence of  $\langle N_c \rangle$  on the target mass  $A_T$  is displayed in **Figure 6** for both  $^{28}\text{Si}$  and  $^{32}\text{S}$  projectiles at 14.6 and 200 AGeV respectively. The values of  $\langle N_c \rangle$  is also found to increase with the increase of target mass. The experimental data, shown in figure may be fitted quite satisfactorily with the relation of the form:

$$\langle N_c \rangle = 13.07 \pm 1.02 A_T^{0.19 \pm 0.03} \quad (4)$$

$$\langle N_c \rangle = 78.94 \pm 1.55 A_T^{0.18 \pm 0.03} \quad (5)$$

### 3.4. Correlations

Multiplicity correlations among the secondary particles produced in nucleus-nucleus collisions have been widely studied which help to investigate the mechanism of particle production. In order to examine the behaviour of multiplicity correlations of secondary particles produced in nucleus-nucleus collisions, we have studied the following correlations in the interactions of  $^{28}\text{Si}$ -Em and  $^{32}\text{S}$ -Em at 14.6 and 200 AGeV respectively.

#### 3.4.1. Dependence of $\langle N_c \rangle$ on $N_x$ ( $x = b, g, h, s$ )

An attempt has been made to investigate the compound multiplicity correlations for  $^{28}\text{Si}$  and  $^{32}\text{S}$ -emulsion interactions at 14.6 and 200 AGeV respectively. **Figure 7(a)**, **Figure 7(b)** represents the dependence of  $\langle N_c \rangle$  on  $N_x$  ( $x = b, g, h, s$ ) for the present data. It may be observed from the figure that  $\langle N_c \rangle$  increases linearly with  $N_b$ ,  $N_g$ ,



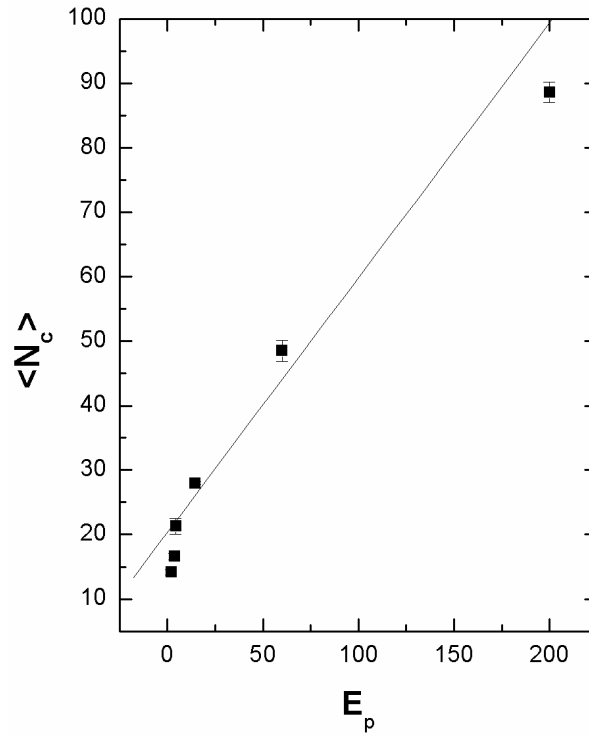


**Figure 5.** Dependence of  $\langle N_c \rangle$  on projectile energy  $E_p$ .

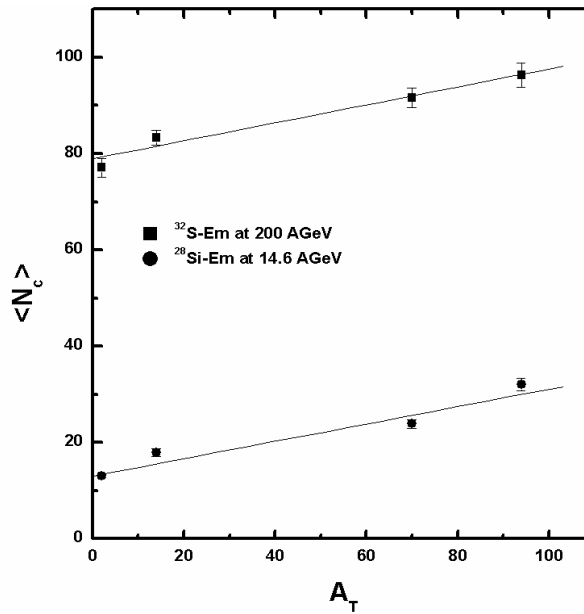


**Figure 6.** Dependence of  $\langle N_c \rangle$  on target size  $A_T$ .

$N_h$  and  $N_s$ . Furthermore, the slopes (inclination),  $k$ , of the linear fits using the least square method are given in [Table 3](#) for the present data. A strong dependence of  $\langle N_c \rangle$  on  $N_b$ ,  $N_g$ ,  $N_h$  and  $N_s$  has been recorded in heavy ion interactions whereas a weak dependence in case of p-nucleus collisions has been reported [3]-[7]. We have also investigated similar multiplicity correlations for the FRITIOF data and values of inclination coefficients,  $k$ , are in good resemblance with those obtained for the experimental data. These values are given in same table in parenthesis along with the respective experimental data.



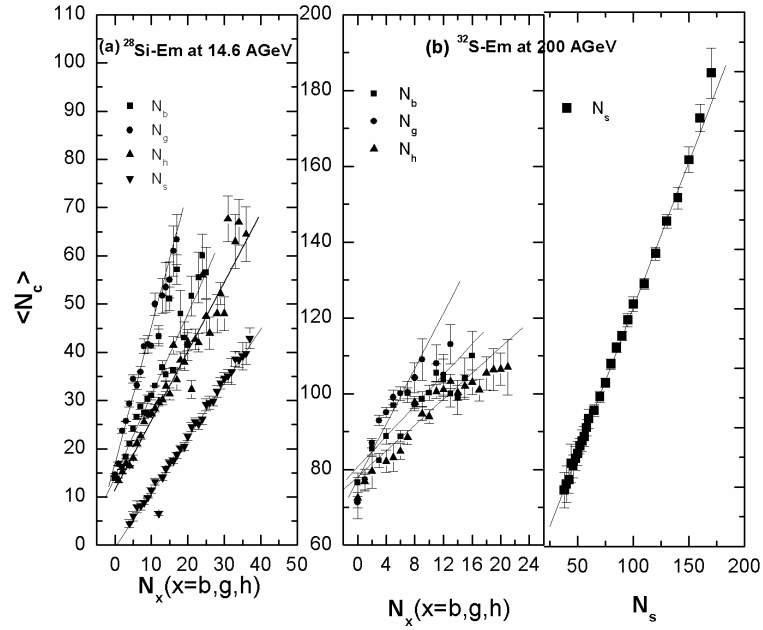


**Figure 7.** Dependence of  $\langle N_c \rangle$  on  $N_b$ ,  $N_g$ ,  $N_h$ ,  $N_s$  in (a)  $^{28}\text{Si}$  and (b)  $^{32}\text{S}$ -emulsion interactions at 14.6 and 200 AGeV.

**Table 3.** Values of inclination coefficients.

Type of correlation	k	
	$^{28}\text{Si}$ at 14.6 AGeV	$^{32}\text{S}$ at 200 AGeV
$\langle N_c \rangle - N_b$	$1.68 \pm 0.07$ ( $5.10 \pm 0.74$ )	$1.76 \pm 0.32$ ( $4.11 \pm 0.56$ )
$\langle N_c \rangle - N_g$	$2.83 \pm 0.18$ ( $2.69 \pm 0.34$ )	$4.68 \pm 0.61$ ( $3.50 \pm 0.22$ )
$\langle N_c \rangle - N_h$	$2.15 \pm 0.13$ ( $3.20 \pm 0.30$ )	$2.11 \pm 0.26$ ( $4.18 \pm 0.31$ )
$\langle N_c \rangle - N_s$	$1.13 \pm 0.04$ ( $1.12 \pm 0.007$ )	$0.98 \pm 0.01$ ( $1.04 \pm 0.03$ )
$\langle N_b \rangle - N_c$	$0.28 \pm 0.007$ ( $0.08 \pm 0.002$ )	$0.02 \pm 0.002$ ( $0.01 \pm 0.001$ )
$\langle N_g \rangle - N_c$	$0.18 \pm 0.006$ ( $0.11 \pm 0.006$ )	$0.03 \pm 0.004$ ( $0.04 \pm 0.001$ )
$\langle N_h \rangle - N_c$	$0.42 \pm 0.005$ ( $0.12 \pm 0.005$ )	$0.06 \pm 0.001$ ( $0.05 \pm 0.002$ )
$\langle N_s \rangle - N_c$	$1.43 \pm 0.08$ ( $0.87 \pm 0.009$ )	$0.91 \pm 0.005$ ( $0.94 \pm 0.006$ )

### 3.4.2. Variation of $\langle N_x \rangle$ ( $x = b, g, h, s$ ) with $N_c$

**Figure 8** shows the correlations between  $\langle N_b \rangle$ ,  $\langle N_g \rangle$ ,  $\langle N_h \rangle$ ,  $\langle N_s \rangle$  and  $N_c$  for  $^{28}\text{Si}$  and  $^{32}\text{S}$  emulsion interactions at 14.6 and 200 AGeV. The experimental results have been analyzed by using linear fits of type  $\langle N_x(N_c) \rangle = c + N_c k$ , where  $N_x = N_b, N_g, N_h, N_s$  and the values of inclination coefficients,  $k$ , are presented in **Table 3**. It is evident from the figures that the values of  $\langle N_b \rangle$ ,  $\langle N_g \rangle$ ,  $\langle N_h \rangle$  and  $\langle N_s \rangle$  increases with increasing values of  $N_c$  in both  $^{28}\text{Si}$  and  $^{32}\text{S}$ -Em at 14.6 and 200 AGeV respectively. The increase of  $\langle N_s \rangle$  with  $N_c$  is much stronger than the others at both energies and projectiles. Here also the inclination coefficients,  $k$ , obtained for the FRITIOF data are in good agreement with the experimental data and are also given in table in parenthesis along with the corresponding experimental data.

### 3.5. KNO Scaling

Asymptotic scaling of multiplicity distributions in hadron collisions was predicted in 1971 by Koba, Nielsen and Olesen [31] by assuming the validity of Feynman scaling [32]. Koba, Nielsen and Olesen have predicted that the multiplicity distributions of the produced particles in high-energy hadron-hadron collisions should obey a simple scaling law known as KNO scaling when expressed in terms of the scaling variable  $Z (=N/\langle N \rangle)$ . If  $P_n(s)$  represents the probability for the production of  $n$  charged particles in an inelastic hadron-hadron collision at a centre of mass energy  $\sqrt{s}$ , then the multiplicity distributions in high energy collision obey a scaling law:

$$P_n(s) = \frac{\sigma_n(s)}{\sigma_{\text{inel}}(s)} = \frac{1}{\langle N \rangle} \Psi\left(\frac{N}{\langle N \rangle}\right) = \frac{1}{\langle N \rangle} \Psi(Z) \quad (6)$$

where  $\sigma_n(s)$  is the partial cross-section for the production of  $n$  charged particles,  $\sigma_{\text{inel}}$  is the total inelastic cross-section and  $\langle N \rangle$  is the average number of charged particles produced. The KNO scaling thus implies that the multiplicity distribution is universal and  $\Psi(Z)$  is an energy independent function at sufficiently high energies when expressed in terms of scaling variable  $Z$ .

It is well established that the KNO scaling is applicable for multiparticle production in hadron-hadron collisions. Many workers have also observed this scaling behaviour in compound multiplicity distribution in nucleus-nucleus collisions at high energies [5] [25]-[27] [30]. It has been shown in Figure 9 that the multiplicity distributions of compound particles,  $N_c$  obtained from the events of  $^{28}\text{Si}$  and  $^{32}\text{S}$  emulsion interactions at 14.6 and 200 AGeV respectively can be described by a KNO scaling law. These distributions can be represented by a universal function of the following form: where  $A$  and  $B$  are constants.

It is easily noticed from the figure that the multiplicity distributions of compound particles,  $N_c$  obtained from the events of  $^{28}\text{Si}$  and  $^{32}\text{S}$  emulsion interactions at 14.6 and 200 AGeV are well described by Equation (7) and seem to satisfy the scaling function. The best values of  $A$  and  $B$  used in Equation (7) are found to be  $4.50 \pm 0.02$  and  $2.05 \pm 0.01$  respectively.

The values of corresponding  $\chi^2/\text{DOF}$  are found to be 0.44 for compound multiplicity which indicates that the experimental data agree fairly well with the universal curve represented by solid curve in figure. The consequences of KNO scaling is also observed in the linear variation of  $D(N_c)$  with  $\langle N_c \rangle$  (Figure 2), which is in accordance with the predictions of KNO scaling. Thus the compound multiplicity distributions for the present data obey KNO scaling, which is independent of mass number and energy of the projectile.

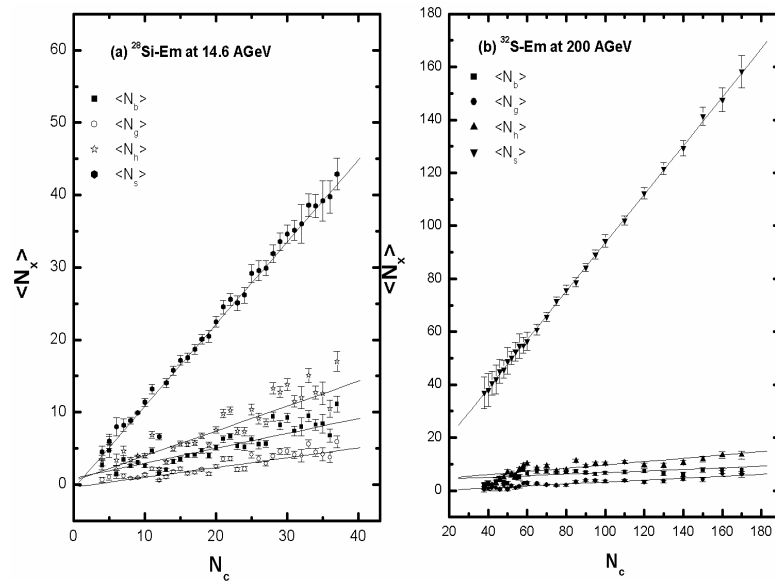


**Figure 8.** Dependence of  $\langle N_b \rangle$ ,  $\langle N_g \rangle$ ,  $\langle N_h \rangle$ ,  $\langle N_s \rangle$  on  $N_c$  in (a)  $^{28}\text{Si}$ -emulsion interactions at 14.6 AGeV and (b)  $^{32}\text{S}$ -emulsion interactions at 200 AGeV.

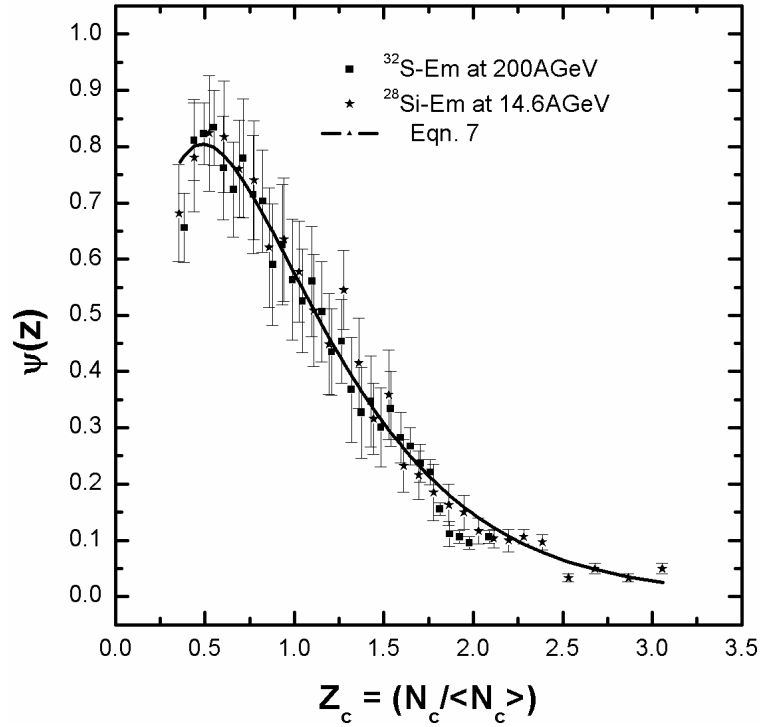


**Figure 9.** Compound particle multiplicity distribution in terms of KNO scaling in  $^{28}\text{Si}$  and  $^{32}\text{S}$ -Em interactions at 14.6 and 200 AGeV.

$$\Psi(z) = AZ \exp(-BZ) \quad (7)$$

#### 4. Conclusion

It may be concluded from the present investigation that the compound multiplicity distributions in the interaction of  $^{28}\text{Si}$  and  $^{32}\text{S}$  projectiles at 14.6 and 200 AGeV respectively with different target groups can be well reproduced by the FRITIOF data. The average compound multiplicity has been found to increase with projectile mass and energy as well with the target size. Also the multiplicity correlation among various secondary particles exhibit linear relation and the experimental values of the inclination coefficients are in fairly good agreement with the FRITIOF data. The compound multiplicity distribution is observed to obey KNO scaling law, for both the projectiles at two different energies showing that the scaling is independent of mass number and energy of the projectile.

#### Acknowledgements

We would like to express our thanks to Professor P.L. Jain of SUNY at Buffalo, USA for providing the exposed and developed emulsion plates for the present analysis. Mir Hashim Rasool acknowledges Dr. Shakil Ahmad for his help in generating events using FRITIOF model.

#### References

- [1] Abd-Allah, N.N. and Mohery, N. (2001) Features of the Compound Multiplicity of the Interactions of  $^{24}\text{Mg}$  and  $^{28}\text{Si}$  Ions with Emulsion Nuclei at 4.5A GeV/c. *Turkish Journal of Physics*, **25**, 109-119.
- [2] Jurak, A. and Linscheid, A. (1977) Some Characteristics of Compound Shower and Grey Tracks Multiplicity Distributions Produced in Proton Emulsion Interactions. *Acta Physica Polonica B*, **8**, 875-886.
- [3] Ahmad, T., *et al.* (2010) Characteristics of Compound Multiplicity in Hadron-Nucleus Collisions. *Indian Journal of Pure and Applied Physics*, **48**, 855-859.
- [4] Ahmad, T. (2014) A Study of Pion-Nucleus Interactions in Terms of Compound Particles. *Advances in High Energy*

*Physics*, **5**, 6.

- [5] Ghosh, D., Mukhopadhyay, A., Ghosh, A., Sengupta, R. and Roy, J. (1989) Multiplicity Characteristics of Heavy-Ion Interactions at 4.5 GeV per Nucleon. *Nuclear Physics A*, **499**, 850-860. [http://dx.doi.org/10.1016/0375-9474\(89\)90067-5](http://dx.doi.org/10.1016/0375-9474(89)90067-5)
- [6] Ahmad, T. and Irfan, M. (1991) Features of Compound Multiplicity in Heavy-Ion Interactions at 4.5A GeV/c. *Physical Review C*, **44**, 1555-1558. <http://dx.doi.org/10.1103/PhysRevC.44.1555>
- [7] Khan, M.S., *et al.* (1997) Some Interesting Results on Compound Multiplicity in <sup>12</sup>C-Nucleus Reactions at 4.5A GeV/c. *Canadian Journal of Physics*, **75**, 549-557. <http://dx.doi.org/10.1139/p97-149>
- [8] Abou-Moussa, Z. (2002) Compound Multiplicity in the Collisions of 4.1A GeV/c <sup>22</sup>Ne Nuclei with Nuclear Emulsion. *Canadian Journal of Physics*, **80**, 109-117. <http://dx.doi.org/10.1139/p01-143>
- [9] Zhang, D.H., He, C.L.Y., *et al.* (2006) Features of Compound Multiplicity in <sup>16</sup>O-Em Interactions at 4.5A GeV/c. *Chinese Journal of Physics*, **44**, 405-417.
- [10] Mohery, M. and Arafa, M. (2011) Some Characteristics of the Compound Multiplicity in High-Energy Nucleus-Nucleus Interactions. *International Journal of Modern Physics E*, **20**, 1735-1754. <http://dx.doi.org/10.1142/S0218301311019532>
- [11] Anderson, B., Gustafson, G. and Nilsson-Almqvist, B. (1987) A Model for Low-pT Hadronic Reactions with Generalizations to Hadron-Nucleus and Nucleus-Nucleus Collisions. *Nuclear Physics B*, **281**, 289-309.
- [12] Nilson-Almqvist, B. and Stenlund, E. (1987) Interactions between Hadrons and Nuclei: The Lund Monte Carlo-FRITIOF Version 1.6. *Computer Physics Communications*, **43**, 387-397. [http://dx.doi.org/10.1016/0010-4655\(87\)90056-7](http://dx.doi.org/10.1016/0010-4655(87)90056-7)
- [13] Bradt, H.L. and Peters, B. (1948) Investigation of the Primary Cosmic Radiation with Nuclear Photographic Emulsions. *Physical Review*, **74**, 1828-1839. <http://dx.doi.org/10.1103/PhysRev.74.1828>
- [14] Barashenkov, V.S., Beliaikov, V.A., Glagolev, V.V., Dalkhazhav, N., Se, Y.T., Kirillova, L.F., *et al.* (1959) Mechanism of Interaction of Fast Protons with Nucleons and Nuclei. *Nuclear Physics*, **14**, 522-539. [http://dx.doi.org/10.1016/0029-5582\(60\)90471-5](http://dx.doi.org/10.1016/0029-5582(60)90471-5)
- [15] Powell, C.F., Flower, P.H. and Perkins, D.H. (1959) The Study of Elementary Particles by Photographic Method. Pergamon Press, London.
- [16] Jakobsson, B. and Kullberg, R. (1976) Interactions of 2 GeV/Nucleon <sup>16</sup>O with Light and Heavy Emulsion Nuclei. *Physica Scripta*, **13**, 327-333. <http://dx.doi.org/10.1088/0031-8949/13/6/002>
- [17] Ahmad, M.A., Rasool, M.H. and Ahmad, S. (2012) General Characteristics of Heavy Ion Collisions at the Energy of 14.6A GeV. *International Journal of Theoretical and Applied Physics*, **2**, 199-220.
- [18] Jain, P.L., Sengupta, K. and Singh, G. (1991) Production of Fast and Slow Particles in Nucleus-Nucleus Collisions at Ultra Relativistic Energies. *Physical Review C*, **44**, 844-856. <http://dx.doi.org/10.1103/PhysRevC.44.844>
- [19] Antonchik, V.A., *et al.* (1980) Some Characteristics of Inelastic Interactions between <sup>56</sup>Fe Nuclei at 0, 5-2 GeV/ Nucleon with Photoemulsion Nuclei. *Soviet Journal of Nuclear Physics*, **32**, 164-172.
- [20] Chernov, G.M., Gulamov, K.G., Gulyamov, U.G., Nasyrov, S.Z. and Svechnikova, L.N. (1977) Interactions of Relativistic Nitrogen Nuclei in an Emulsion at 2.1 GeV/Nucleon. *Nuclear Physics A*, **280**, 478-490. [http://dx.doi.org/10.1016/0375-9474\(77\)90616-9](http://dx.doi.org/10.1016/0375-9474(77)90616-9)
- [21] Barashenkov, V.S. and Toneev, V.D. (1972) Interactions of High Energy Particles and Nuclei with Nuclei. Atomizdat, Moscow.
- [22] Gottfried, K. (1974) Space-Time Structure of Hadronic Collisions and Nuclear Multiple Production. *Physical Review Letters*, **32**, 957-961. <http://dx.doi.org/10.1103/PhysRevLett.32.957>
- [23] Ghosh, D., Mukhopadhyay, A., Ghosh, A., Sengupta, R. and Roy, J. (1989) Multiplicity Characteristics of Heavy-Ion Interactions at 4.5 GeV/yc per Nucleon. *Nuclear Physics A*, **499**, 850-860. [http://dx.doi.org/10.1016/0375-9474\(89\)90067-5](http://dx.doi.org/10.1016/0375-9474(89)90067-5)
- [24] El-Daiem, A. (2010) Characteristics of Compound Multiplicity in <sup>24</sup>Mg with Emulsion at 4.5 AGeV/c. *Physics International*, **1**, 31-37. <http://dx.doi.org/10.3844/pisp.2010.31.37>
- [25] Basova, E.S., Chernov, G.M., Gulamov, K.G., Gulyamov, U.G. and Rakhimbaev, B.G. (1978) A Study of Inelastic Interactions of Deuterons and Alphas in an Emulsion at Approximately. 3.6-GeV/Nucleon. *Zeitschrift fur Physik A Atoms and Nuclei*, **287**, 393-405. <http://dx.doi.org/10.1007/BF01481722>
- [26] El-Nadi, M., Uzhinskii, V.V., Sherif, M.M., Abd-Elsalam, A., El-Nagdy, M.S., Yasin, M.N., *et al.* (2004) Some Characteristics of <sup>6</sup>Li and <sup>7</sup>Li Isotopes Interactions with Emulsion Nuclei at 3.7-4.5 AGeV/c. *International Journal of Modern Physics E*, **13**, 619.
- [27] Bai, C.Y. and Zhang, D.-H. (2011) Study of Compound Particle Production in <sup>84</sup>Kr-Emulsion Interactions at 1.7A GeV.

- Chinese Physics C*, **35**, 349-354. <http://dx.doi.org/10.1088/1674-1137/35/4/006>
- [28] Ghosh, D., Roy, J. and Sengupta, R. (1987) Study of Multiparticle Production in the Interaction of  $^{12}\text{C}$  with Photo-Emulsion Nuclei at 4.5 GeV/c. *Nuclear Physics A*, **468**, 719-738. [http://dx.doi.org/10.1016/0375-9474\(87\)90190-4](http://dx.doi.org/10.1016/0375-9474(87)90190-4)
- [29] Ghosh, D., Mukhopadhyay, A., Ghosh, A., Sengupta, R. and Roy, J. (1989) Multiplicity Characteristics of Heavy Ion Interactions at 4.5 GeV/yc per Nucleon. *Nuclear Physics A*, **499**, 850-860. [http://dx.doi.org/10.1016/0375-9474\(89\)90067-5](http://dx.doi.org/10.1016/0375-9474(89)90067-5)
- [30] Chouhan, N.S., Singh, M.K., Singh, V. and Pathak, R. (2013) Characteristics of Compound Multiplicity in  $^{84}\text{Kr}_{36}$  with Various Light and Heavy Targets at 1 GeV per Nucleon. *Indian Journal of Physics*, **87**, 1263-1267. <http://dx.doi.org/10.1007/s12648-013-0366-5>
- [31] Koba, Z., Nielsen, H.B. and Olesen, P. (1972) Scaling of Multiplicity Distributions in High Energy Hadron Collisions. *Nuclear Physics B*, **40**, 317-334. [http://dx.doi.org/10.1016/0550-3213\(72\)90551-2](http://dx.doi.org/10.1016/0550-3213(72)90551-2)
- [32] Feynman, R.P. (1969) Very High-Energy Collisions of Hadrons. *Physical Review Letters*, **23**, 1415-1417. <http://dx.doi.org/10.1103/PhysRevLett.23.1415>